# BEST AVAILABLE IMAGES

Defective images within this document are accurate representations of the original documents submitted by the applicant.

Defects in the images may include (but are not limited to):

- BLACK BORDERS
- TEXT CUT OFF AT TOP, BOTTOM OR SIDES
- FADED TEXT
- ILLEGIBLE TEXT
- SKEWED/SLANTED IMAGES
- COLORED PHOTOS
- BLACK OR VERY BLACK AND WHITE DARK PHOTOS
- GRAY SCALE DOCUMENTS

## IMAGES ARE BEST AVAILABLE COPY.

**As rescanning documents *will not* correct images, please do not report the images to the Image Problem Mailbox.**

**STIC-ILL**

QH573.C95
Adams

**From:** Canella, Karen
**Sent:** Thursday, January 09, 2003 6:41 PM
**To:** STIC-ILL
**Subject:** ill order 09/872,364

Art Unit 1642 Location 8E12(mail)

Telephone Number 308-8362

Application Number 09/872,364

1. FEBS Lett:
   1994, 351(2):211-214
   1994, 341(2-3):277-280

2. Biochemistry, 1993, Vol. 32, pp. 1212-1218

3. PNAS, 1994, Vol. 91, pp. 12501-12504

4. Gene:
   1992, Vol. 111, pp. 229-233
   1996, Vol. 173, pp. 33-38

5. Cytometry, 1995 Dec 1, 21(4):309-317

6. Focus, 1996, 18(2):40-43

Cytometry 21:309–317 (1995)

Rapid Communication

# *Aequorea* Green Fluorescent Protein Analysis by Flow Cytometry

**J. Dezz Ropp, Christopher J. Donahue, David Wolfgang-Kimball, Jeffrey J. Hooley, James Y.W. Chin, Robert A. Hoffman, R. Andrew Cuthbertson, and Kenneth D. Bauer**

Departments of Pulmonary Research (J.D.R., R.A.C.) and Immunology (C.J.D., D.W.-K., J.J.H., J.Y.W.C., K.D.B.), Genentech, Inc., South San Francisco, and Becton-Dickinson Immunocytometry Systems, San Jose (R.A.H.), California

Received for publication July 17, 1995; accepted September 5, 1995

**The isolation and expression of the cDNA for the green fluorescent protein (GFP) from the bioluminescent jellyfish *Aequorea victoria* has highlighted its potential use as a marker for gene expression in a variety of cell types (Chalfie et al.: Science 263: 802–805, 1994). The longer wavelength peak (470 nm) of GFP's bimodal absorption spectrum better matches standard fluorescein filter sets; however, it has a considerably lower amplitude than the major absorption peak at 395. In an effort to increase the sensitivity of GFP with routinely available instrumentation, Heim et al. (Nature 373:663–664, 1995) have generated a GFP mutant (serine-65 to threonine; S65T-GFP) which possesses a single absorption peak centered at 490 nm. We have constructed this mutant in order to determine whether it or wild-type GFP (wt-GFP) afforded greater sensitivity when excited near their respective absorption maxima. Using the conventionally available 488 nm and ultraviolet (UV) laser lines from the argon ion laser as well as the 407 nm line from a krypton ion laser with enhanced violet emission, we were able to closely match the absorption maxima of both the S65T and wild-type forms of *Aequorea* GFP and analyze differences in fluorescence intensity of transiently transfected 293 cells with flow cytometry. The highest fluorescence signal was observed with 488 nm excitation of S65T-GFP relative to all other laser line/GFP pairs. The wt-GFP fluorescence intensity, in contrast, was significantly higher at 407 nm relative to either 488 nm or UV. These results were consistent with parallel spectrofluorometric analysis of the emission spectrum for wt-GFP and S65T-GFP. The relative contribution of cellular autofluorescence at each wavelength was also investigated and shown to be significantly reduced at 407 nm relative to either UV or 488 nm.**



**Key terms: Green fluorescent protein, flow cytometry, gene expression, autofluorescence, spectrofluorometry, transient transfection**

The unusual spectral properties of the green fluorescent protein (GFP) are responsible for green light emission from the hydromedusan jellyfish *Aequorea victoria* (12). In vivo, GFP is excited by energy transfer from the $Ca^{2+}$-dependent blue light emission of the photoprotein aequorin (11, 20). A similar mechanism involving energy transfer from a photoprotein to a GFP has been demonstrated in a number of other bioluminescent coelenterates (5, 17–19). The covalently-bound *p*-hydroxybenzylidene-imidazolidinone chromophore responsible for the fluorescence of *Aequorea* GFP is derived from the cyclization of the amino acid residues Ser-dehydro Tyr-Gly (4). This $O_2$-dependent cyclization reaction proceeds via a poorly understood mechanism which appears to be either autocatalytic, or at least catalyzed by ubiquitous enzymes, as functional GFP can be expressed in both prokaryotic and eukaryotic cells (3, 10). The GFP spectrum displays a major absorption peak at 395 nm and a minor peak at 470 nm. The fluorescence emission spectrum exhibits a major peak at 509 nm with a shoulder at 540 nm (18, 20, 29).

Although *Aequorea* GFP has been identified and studied extensively since the late 1960s, recent isolation of the cDNA (22) and its subsequent expression in heterologous cell types (3, 10) has opened a new chapter for this protein as a marker for gene expression. The intrinsic

Address reprint requests to Dr. Kenneth D. Bauer, MS#50, 460 Pt. San Bruno Blvd., South San Francisco, CA 94080.

fluorescence of GFP allows detection in living cells obviating the need for fixing the cells or adding a chromatic substrate or antibody. The capability to express GFP as a fusion protein has further demonstrated the utility of GFP as a marker for subcellular localization (2, 7, 15, 16, 21, 28).

Routinely available filters and lasers used for detecting fluorescein are the most convenient and obvious choice for detecting GFP expression. The lower amplitude of the 470 nm absorption peak in the GFP spectrum is, however, potentially limiting for optimal detection of the protein. Recently, mutant forms of GFP have been generated which alter the spectral properties of the protein (6, 8, 9). A single point mutation replacing serine-65 with a threonine (S65T-GFP) has been described, which shifts the absorption spectrum to a single peak with a maximum at 490 nm (8). The similarity of spectral characteristics between this mutant form of GFP and fluorescein has been postulated to facilitate higher sensitivity detection of GFP using routinely available fluorescein-designed filter sets. Conversely, increased sensitivity could be achieved by a more appropriate excitation of wild-type GFP (wt-GFP) near its 395 nm absorption maxima.

We have constructed the S65T-GFP mutant in order to compare the sensitivity of detection near its maximal excitation wavelength (488 nm) with detection of wt-GFP at excitation wavelengths near its maxima (355 nm, 407 nm). By assaying transient expression of wt-GFP and S65T-GFP in 293 cells by flow cytometry, our results have clearly demonstrated an optimal analysis scheme for the detection of GFP expression in eukaryotic cells. Further analysis with respect to cellular autofluorescence at these wavelengths has indicated potential advantages of the 407 nm laser line for other applications.

## MATERIALS AND METHODS

### Reagents

Opti-MEM, Lipofectin, trypsin-EDTA, and DH5α competent *Escherichia coli* cells were purchased from Gibco BRL Life Technologies (Gaithersburg, MD) and used according to manufacturer's recommendations. 7-amino actinomycin D (7-AAD) was obtained from Calbiochem (San Diego, CA). Oligonucleotides were synthesized on an ABI 394 DNA synthesizer (Foster City, CA). Restriction enzymes and T4 DNA ligase were purchased from Gibco BRL Life Technologies and New England Biolabs (Beverly, MA). *TaKaRa Ex Taq* DNA polymerase was obtained from PanVera Corp (Madison, WI). Recombinant GFP protein and anti-rGFP antiserum were purchased from Clontech Laboratories (Palo Alto, CA). Tris-glycine polyacrylamide gels and PVDF membranes were from NOVEX (San Diego, CA). A pBluescript II KS (+) derivative, pTU65 (3), was the source of the cDNA encoding wt-GFP.

### Cell Lines

293 Cells, a human embryonal kidney line (ATCC CRL 1573), were maintained in high-glucose DMEM/F-12 media supplemented with 10% heat inactivated fetal bovine serum (HIFBS) at 37°C/5% $CO_2$.

### DNA Manipulations and Mutagenesis

The wt-GFP gene was amplified from pTU65 (3) with primers which generated an *Eco*RI and a *Bam*HI site flanking the respective ends of the gene for insertion into an expression vector under control of the CMV promoter (pCMV). This construct, pCMV.gfp, was used for expression of the wt-GFP. The S65T-GFP mutant (8) was constructed by PCR amplification of the gene from pCMV.gfp in two overlapping fragments centered on amino acid position 65. Within the overlapping region, the S65T mutation was engineered (TCT→ACT; double underline below) in the 3′-fragment, along with two silent point mutations (single underline below) which generated a unique *Bst*EII site in both the 3′- and 5′-fragments (internal GFP oligos 5′-ACACTGGTCACCACTTTCACTTAT-3′ and 5′AGAGAAA-GTGGTGACCAGTGT-3′, respectively). This unique site facilitated reassembly of the two mutant gene fragments into the parental pCMV expression vector. This construct, pCMV.S65T-gfp, was the source of S65T-GFP expression. Plasmid DNA was propagated in DH5α competent cells. All DNA used for transfections was purified by CsCl centrifugation. All other standard DNA manipulations were according to Sambrook et al. (23).

### Transient Transfections

293 Cells were plated at $2 \times 10^5$ cells per well in 6-well plates (Corning, Corning, NY) and grown for 24–30 h (~30–40% confluency). DNA-Lipofectin complexes were formulated by mixing equal volumes of Lipofectin and DNA in Opti-MEM (at stock concentrations of 8 μl/100 μl and 140 fmol/100 μl, respectively, per $2 \times 10^5$ cells) for 15 min at room temperature. The complexes were diluted 5-fold with Opti-MEM and 1 ml of the mix added to cells pre-rinsed with PBS. Incubation was performed for 8–12 h at 37°C/5% $CO_2$. Cells were then supplemented with 0.5 volumes high-glucose DMEM/F-12/30% HIFBS, for a final serum concentration of 10%, and incubated for an additional 12–24 h at 37°C/5% $CO_2$. Cells were detached from the wells by trypsin-EDTA treatment (200 μl, 1 × concentration; 5 min, RT), harvested into high-glucose DMEM/F-12/10% HIFBS (1 ml/well) and pelleted (500*g*, 10 min; Beckman GS-6 tabletop centrifuge). For analysis by flow cytometry, the cells were resuspended in 5% FBS, 0.1 mM EDTA, 2 μg/ml 7-AAD in PBS at ~$1 \times 10^6$ cells/ml; for spectrofluorometry measurements, 7-AAD was omitted. Cell sorting was performed on cells pooled from 24 replicate transfections of $2 \times 10^5$ cells/transfection for each vector construct. Parallel transfections were conducted for wt-GFP (pCMV.gfp), S65T-GFP (pCMV.S65T-gfp) as well as a mock transfection with the parental pCMV vector; in all cases fluorescence intensity measurements were referenced to untransfected 293 cells treated in a similar manner.

### Western Analysis

Transfected cells (100 k each) were pelleted and resuspended in 20 μl 1 × SDS loading buffer containing 5% β-mercaptoethanol. Samples were heated at 95°C for 5

min and then vigorously vortexed to shear high-molecular weight DNA. The heated samples were immediately loaded onto a 12% acrylamide Tris-glycine gel (13). After electrophoresis, the gel was soaked in Towbin buffer (27) and blotted onto a PVDF membrane using the Xcell II blot module (NOVEX). The blotted membrane was then blocked with phosphate buffered saline (PBS) containing 5% nonfat dry milk, 2% BSA, 0.1% gelatin, and 0.2% Tween 20 for 1 h at room temperature. Incubation of the membrane with anti-rGFP antiserum at 1:2,000 dilution in blocking buffer was performed for 1 h at room temperature. The membrane was then washed extensively (5 × 5 min) with PBS/5% nonfat dry milk/0.1% gelatin/0.2% Tween 20. HRP-conjugated goat anti-rabbit IgG (Biosource, Camarillo, CA) was diluted 1:20,000 with PBS/5% nonfat dry milk/0.1% gelatin/0.2% Tween 20 for the secondary incubation (1 h, room temperature). After washing with PBS/0.1% gelatin/0.05% Tween 20 (6 × 5 min), the ECL substrate (Amersham, Arlington Heights, IL) was added according to manufacturer's recommendation. After addition of substrate, the membrane was exposed to X-ray film for 1 min. Densitometric analysis of the autoradiogram was performed with Whole Band Analyzer version 3.2 (Bio Image, Ann Arbor, MI).

### Flow Cytometry Analysis and Sorting

Flow cytometric analysis and sorting were performed using an EPICS Elite-ESP cytometer (Coulter Corp., Hialeah, FL) equipped with Spectrum argon ion-krypton ion mixed-gas and Innova 302 krypton ion lasers (Coherent, Inc., Santa Clara, CA). The Innova 302 laser (which has enhanced ultraviolet and violet output) was tuned to 407 nm, 50 mW, and the Spectrum mixed-gas laser was tuned to either 488 nm, 50 mW, or to multiline ultraviolet (UV; 351–355 nm) at the same power. Laser power was verified in each experiment using a Fieldmaster laser power meter (Coherent).

The emission of wt-GFP, S65T-GFP, and green cellular autofluorescence (500–550 nm) was measured at each excitation wavelength using the combination of a 550 nm dichroic long-pass filter and a 525 ± 25 nm bandpass filter along with the appropriate laser blocking filter for each excitation line: At 488 nm, a 488 nm laser-blocking long-pass filter was used, whereas a 430 nm laser-blocking longpass filter (Chroma Technology Corp., Brattleboro, VT) was used with multiline UV or 407 nm excitation. Utilization of the 525 ± 25 nm bandpass filter was found to give superior wt-GFP and S65T-GFP detection relative to 495, 505, or 515 nm long-pass filters (data not shown). In some experiments blue cellular autofluorescence (440–475 nm) was also measured by the addition of 475 nm dichroic long-pass and 460 ± 20 nm bandpass filters in the optical path. 7-AAD fluorescence was collected from a second photomultiplier by the addition of a 665 nm long-pass filter after the long-pass dichroic (Omega Optical, Brattleboro, VT). DNA check microspheres (Coulter Corp.) were used to align the instrument in each experiment.

Cell sorting for both wt-GFP and S65T-GFP was performed using 488 nm excitation, 50 mW with a 1-droplet sort at a flow rate of 3,000 cells/sec. The sort region used to select GFP-expressing cells was set based on pCMV mock-transfected cells such that less than 1% of fluorescence from the mock sample was in the sort region. Viable cells transiently expressing GFP were sorted based on the absence of detectable incorporation of 7-AAD. The average sorting purity was 95% for wt-GFP and 96% for S65T-GFP.

### Spectrofluorometry

Fluorescence emission spectra of transiently transfected cells were obtained using either an SLM 4800C or SLM 8100 spectrofluorometer (SLM Instruments, Inc., Urbana, IL). The light source was a Xenon arc lamp, the output of which was passed through a monochromator and filter to illuminate a quartz cuvette containing the sample. The excitation monochromator bandwidth setting was 2 nm and bandpass filters centered at each excitation wavelength were placed in the excitation path to reduce scattered light that could enter the emission monochromator. The emission monochromator bandwidth was set at 8 nm. For 400 and 488 nm excitation, a 420 nm sharp cut long-pass or KV500 long-pass filter, respectively, was placed in front of the emission monochromator. No filter was used in the emission path for 350 nm excitation. Spectra were acquired to the instrument's computer with a resolution of 1 nm/channel. The digital spectral data were converted to ASCII format for further analysis and plotting. A solution of fluorescein isothiocyanate-conjugated protein was used to check the emission spectrum calibration. A suspension of non-fluorescent chicken erythrocytes fixed with 2% osmium tetraoxide ($OsO_4$ CRBC; Riese Enterprises, San Jose, CA) was used to estimate baseline noise in the emission spectra (14). All cell suspensions were analyzed at a concentration of approximately $1 \times 10^7$/ml.

### Statistical Analysis

Statistical analysis was performed on log fluorescence intensity values using a two-way analysis of variance with experiment and experimental groups used as factors. Log intensity was used to improve homogeneity of variance within the dataset. For statistical analysis of the fraction of cells expressing detectable levels of wt-GFP or S65T-GFP at 488 nm excitation, a paired t-test was performed. Differences were considered significant if $P < 0.05$.

## RESULTS

### Autofluorescence

Previous solution studies of wt-GFP indicate a bimodal absorption curve with the major absorption maximum at approximately 395 nm and a second absorption peak at 470 nm (18, 20, 29). Since cellular autofluorescence has been shown to be a limiting factor for the detection of weak cellular fluorescence following excitation in the blue/violet/ultraviolet region of the spectrum (24), initial studies were undertaken to better assess the extent of cellular autofluorescence following excitation at either

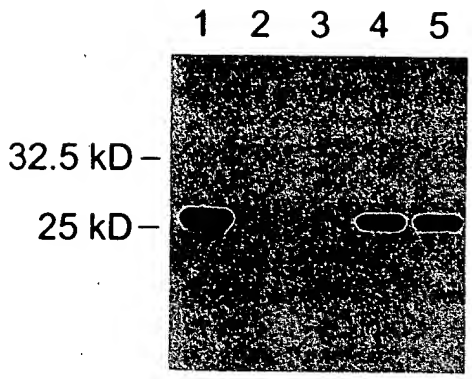


FIG. 1. Measurement of green (500–550 nm) and blue (440–475 nm) relative cellular autofluorescence as a function of laser wavelength. 293 Cells were measured by flow cytometry using UV (351–355 nm), 407 nm, or 488 nm laser excitation and fluorescence intensity was compared to that of osmium tetraoxide-fixed chicken red blood cells (CRBC). The plotted values represent mean linear fluorescence of the 293 cells ÷ mean linear fluorescence of CRBC at the same instrument settings; CRBC values presumably are an indicator of background light scatter. Error bars represent standard errors of the mean. For green autofluorescence results at 488 and 407 nm, n = 5; whereas, for UV, n = 3. Blue autofluorescence results are based on two experiments for all excitation wavelengths. Significant differences in green autofluorescence were observed for both UV and 488 nm excitation relative to 407 nm ($P < 0.001$). Differences in blue autofluorescence were also significant for UV as compared to 407 nm excitation ($P < 0.001$).

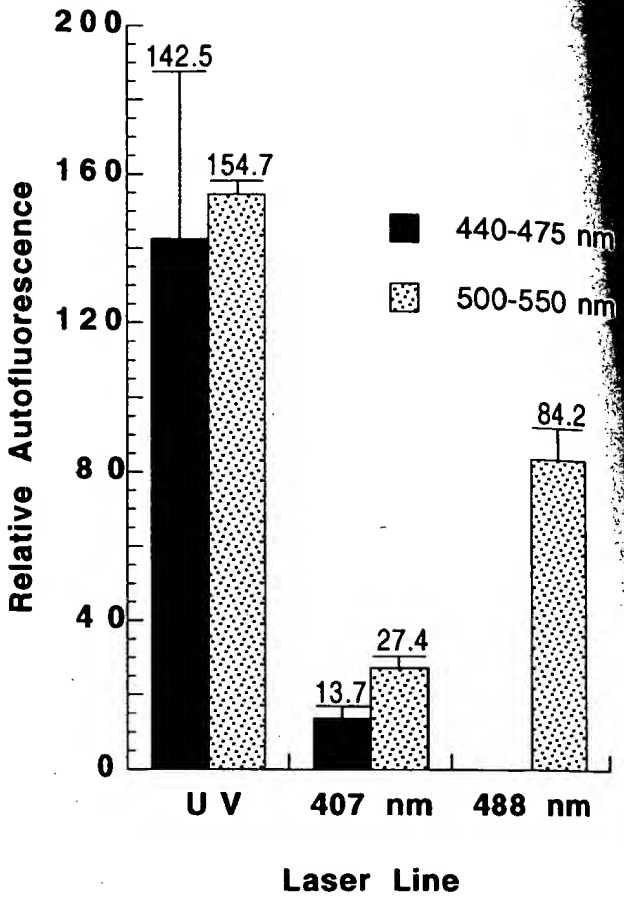


FIG. 2. Western analysis of cell lysates with anti-rGFP antiserum. *Lane 1,* 20 ng purified rGFP; *lane 2,* 293 cells; *lane 3,* 293 cells transfected with pCMV; *lane 4,* 293 cells transfected with pCMV.gfp; *lane 5,* 293 cells transfected with pCMV.S65T-gfp (lanes 2–5 contain 100,000 cells each).

UV, 407 nm, or 488 nm. Osmium tetraoxide-fixed CRBC served as an autofluorescence control for measurement of the background autofluorescence of 293 cells at each wavelength (14). Figure 1 demonstrates the significant variation in the magnitude of relative cellular autofluorescence observed between the three excitation wavelengths when examined in the green or blue spectral regions. A 5.6-fold higher green autofluorescence was observed with UV relative to 407 nm excitation, whereas a 3-fold increase was detected with 488 nm relative to 407 nm excitation in the same region. Blue autofluorescence was also markedly reduced with 407 nm excitation relative to UV. Similar trends in relative autofluorescence as a function of laser excitation wavelength were observed for MCF-7 (ATCC HTB 22; human breast adenocarcinoma), SW480 (ATCC CCL 228; human colon adenocarcinoma), HeLa (ATCC CCL 2; human cervix epitheloid carcinoma), and NIH/3T3 (ATCC CRL 1658; Swiss mouse embryo) cell lines as well as human lung microvascular endothelial cells and peripheral blood leucocytes (data not shown). The reduced background cellular autofluorescence at 407 nm indicated its potential utility as a more optimal wavelength for the excitation of wt-GFP.

## Western Analysis

293 Cells transiently transfected with either pCMV, pCMV.gfp, or pCMV.S65T-gfp were initially evaluated for GFP expression by Western analysis. A single band is present in the pCMV.gfp and pCMV.S65T-gfp transfected lanes consistent with expression of wt-GFP and S65T-GFP (Fig. 2). Scanning densitometry of Figure 2 also demonstrates that the integrated intensity value of the band in lane 5 (S65T-GFP) is 97% that of lane 4 (GFP).

## Spectrofluorometry

To provide a foundation for subsequent quantitative fluorescence measurements by flow cytometry, spectrofluorometry was employed using pCMV.gfp-, pCMV.S65T-gfp-, and pCMV mock-transfected 293 cells. Fluorescence emission spectral information pertinent to the argon and krypton laser excitation lines available for flow cytometry was collected using fluorescence excitation at 350, 400, and 488 nm. Fluorescence emission spectra were recorded between 350 and 600 nm as appropriate (Fig. 3). With 350 nm excitation, all 293 cells demonstrated a broad emission peak centered at approximately 450 nm. Cells transfected with pCMV.gfp, however, appeared to demonstrate a bimodal fluorescence emission spectrum, with a second fluorescence emission

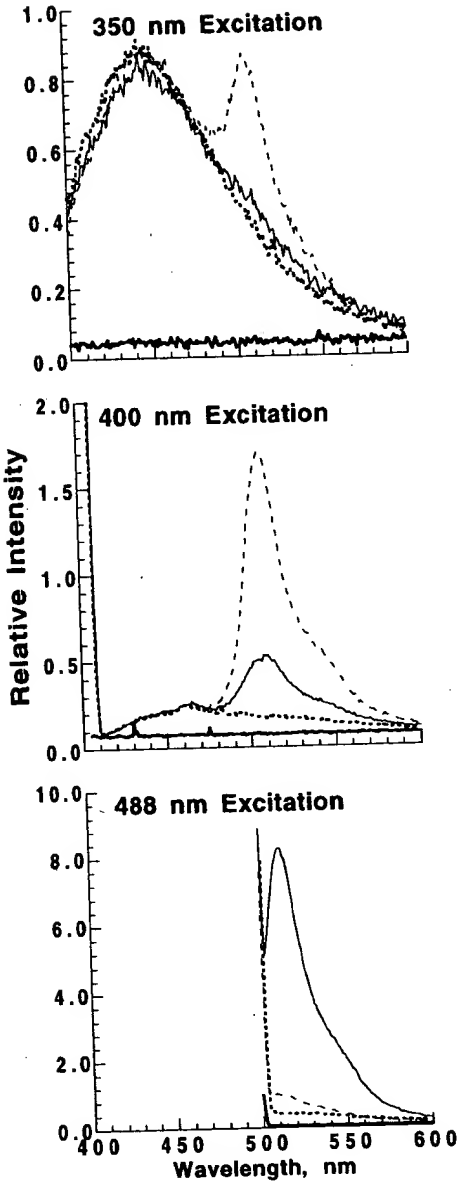


FIG. 3. Fluorescence emission spectra for 293 cells (- - - -), 293 cells transiently transfected with pCMV.gfp (– – – –), 293 cells transiently transfected with pCMV.S65T-gfp (———) and osmium tetraoxide fixed CRBC (———) following excitation at 350, 400, or 488 nm.

peak centered at approximately 510 nm which was not apparent in either the pCMV.S65T-gfp or pCMV mock-transfected 293 cells. For 400 nm excitation, the emission peak at 510 nm was predominant for both wt-GFP and S65T-GFP, with a higher fluorescence emission intensity observed for wt-GFP relative to S65T-GFP. Excitation at 488 nm, in contrast, demonstrated a marked increase in the intensity of the 510 nm emission peak for S65T-GFP which was consistent with enhanced fluorescence of S65T-GFP relative to wt-GFP at this excitation wavelength (8). Measurement of $OsO_4$ CRBC in all cases was unaffected by closing the shutter in front of the emission monochromator, indicating undetectable autofluorescence in these cells.

### Flow Cytometry

Cell sorting and flow cytometry analysis were used to further characterize the fluorescence of wt-GFP- and S65T-GFP-expressing cells using UV, 407 nm, and 488 nm excitation. For these studies, 293 cells transiently transfected with either pCMV.gfp or pCMV.S65T-gfp were analyzed at 488 nm; expressing cells were sorted using pCMV mock-transfected cells as a non-expressing control. The average sorting purity was 95% for wt-GFP and 96% for S65T-GFP. An example of results obtained is shown in Figure 4. Histograms illustrating the fluorescence profiles obtained with 488 nm excitation prior to cell sorting are shown in Figure 4A. The presence of wt-GFP- and S65T-GFP-expression following transfection is detectable in approximately 27 and 50% of cells, respectively, when compared to pCMV mock-transfected cells (values represent an average of five experiments). A significantly higher fraction of positive cells was consistently observed in the pCMV.S65T-gfp-transfected cells relative to the pCMV.gfp-transfected cells ($P = 0.0002$). In the S65T-GFP-expressing cells, excitation at 488 nm resulted in a very broad fluorescence intensity range—extending into the fourth decade relative to pCMV mock-transfected cells.

In Figure 4, examples of histograms obtained by reanalysis of sorted wt-GFP- and S65T-GFP-expressing cells (left and right panels, respectively) with 488 nm (Fig. 4B), 407 nm (Fig. 4C), or 355 nm (Fig. 4D) excitation are shown. Enhanced fluorescence of wt-GFP relative to S65T-GFP was noted for the UV- and 407 nm-excited cells, whereas elevated fluorescence intensity of the S65T-GFP, relative to wt-GFP, was apparent with 488 nm excitation.

Figure 5 provides a summary of normalized fluorescence intensity data for 293 cells, pCMV mock-transfected cells, and for sorted wt-GFP- and S65T-GFP-expressing cells. In each case, the fluorescence values are reported as the linear mean and normalized so that the fluorescence of 293 cells is adjusted to one unit. A significantly higher fluorescence intensity was observed for wt-GFP-expressing cells at 407 nm relative to 488 nm. By contrast, S65T-GFP fluorescence is approximately 16-fold higher at 488 vs. 407 nm. The combination of 488 nm excitation and S65T-GFP expression significantly exceeds all other protein and laser excitation combinations we measured.

## DISCUSSION

By directly comparing the fluorescence intensities of wt-GFP and S65T-GFP elicited by excitation at wavelengths near their respective absorption maxima, we have shown that 488 nm excitation of the S65T-GFP mutant results in significantly enhanced cellular fluorescence relative to all other protein and laser combinations we measured. Confirmation of this observation as deter-

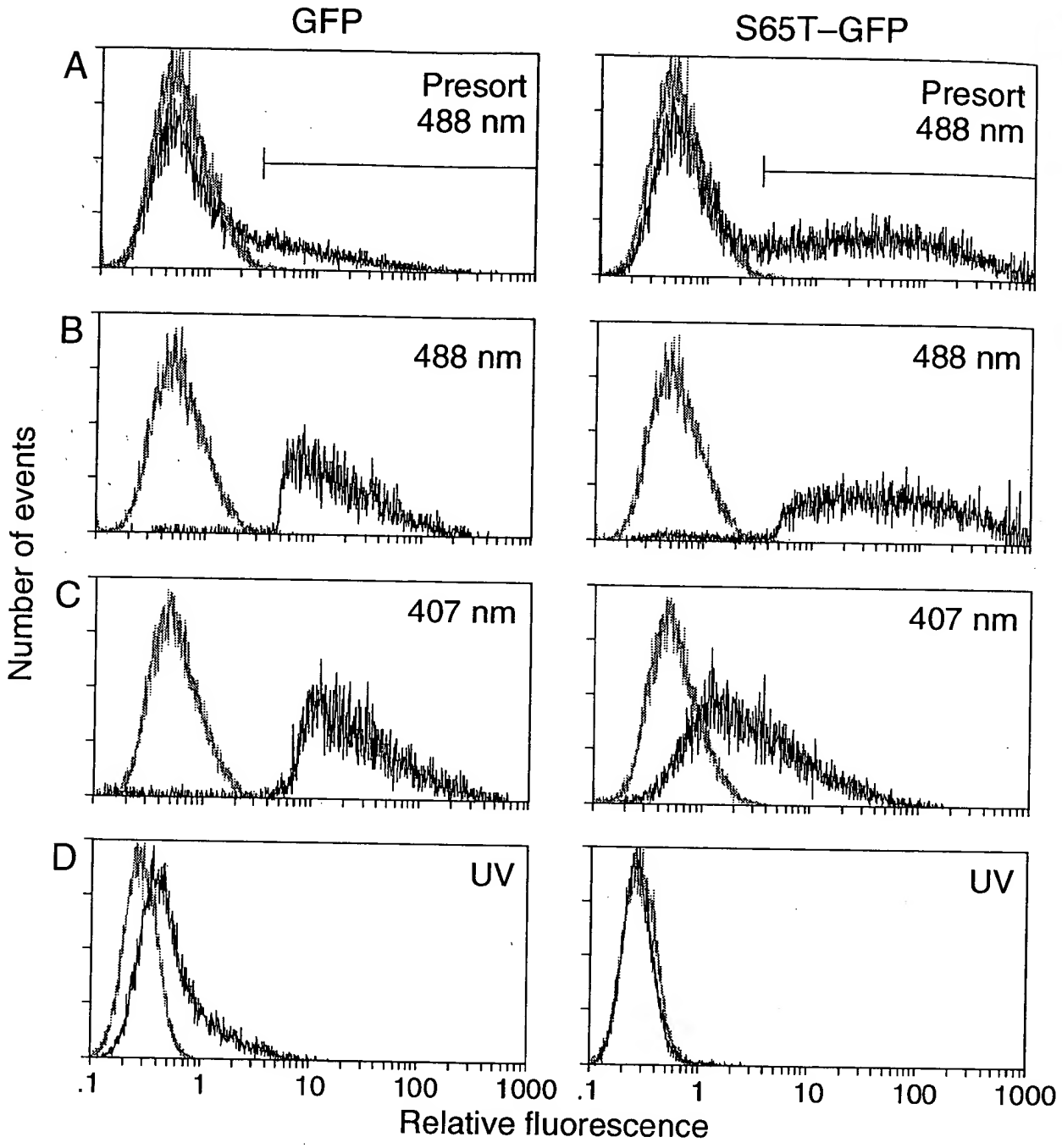


FIG. 4. Flow cytometry histograms for 293 cells. A: Fluorescence histograms for cells transiently transfected with pCMV.gfp (left panels) or pCMV.S65T-gfp (right panels), using 488 nm excitation, are shown prior to cell sorting. The sort regions used for the selection of expressing cells relative to pCMV mock-transfected controls are indicated. Post-sort analysis of wt-GFP- and S65T-GFP-expressing cells following (B) 488 nm, (C) 407 nm, and (D) UV excitation are indicated. In all histograms the pCMV mock-transfected cells are shown in shaded lines for comparison. Nontransfected 293 cells were first analyzed at each excitation wavelength and the instrument adjusted so that reanalysis of the nontransfected cells resulted in a mean fluorescence intensity value of 0.35, thus keeping autofluorescence constant for each excitation wavelength.

mined by flow cytometry was achieved by spectrofluorometric measurements.

The increase in fluorescence intensity of S65T-GFP relative to wt-GFP at 488 nm was not unexpected based on the initial report of this mutation (8). Serine 65 is the serine residue of the Ser-dehydroTyr-Gly triplet which cyclizes to form the *p*-hydroxybenzylidene-imidazolidinone chromophore. When serine-65 is mutated to a threonine, the resulting spectral properties of S65T-GFP are more similar to fluorescein (8). It was hypothesized by

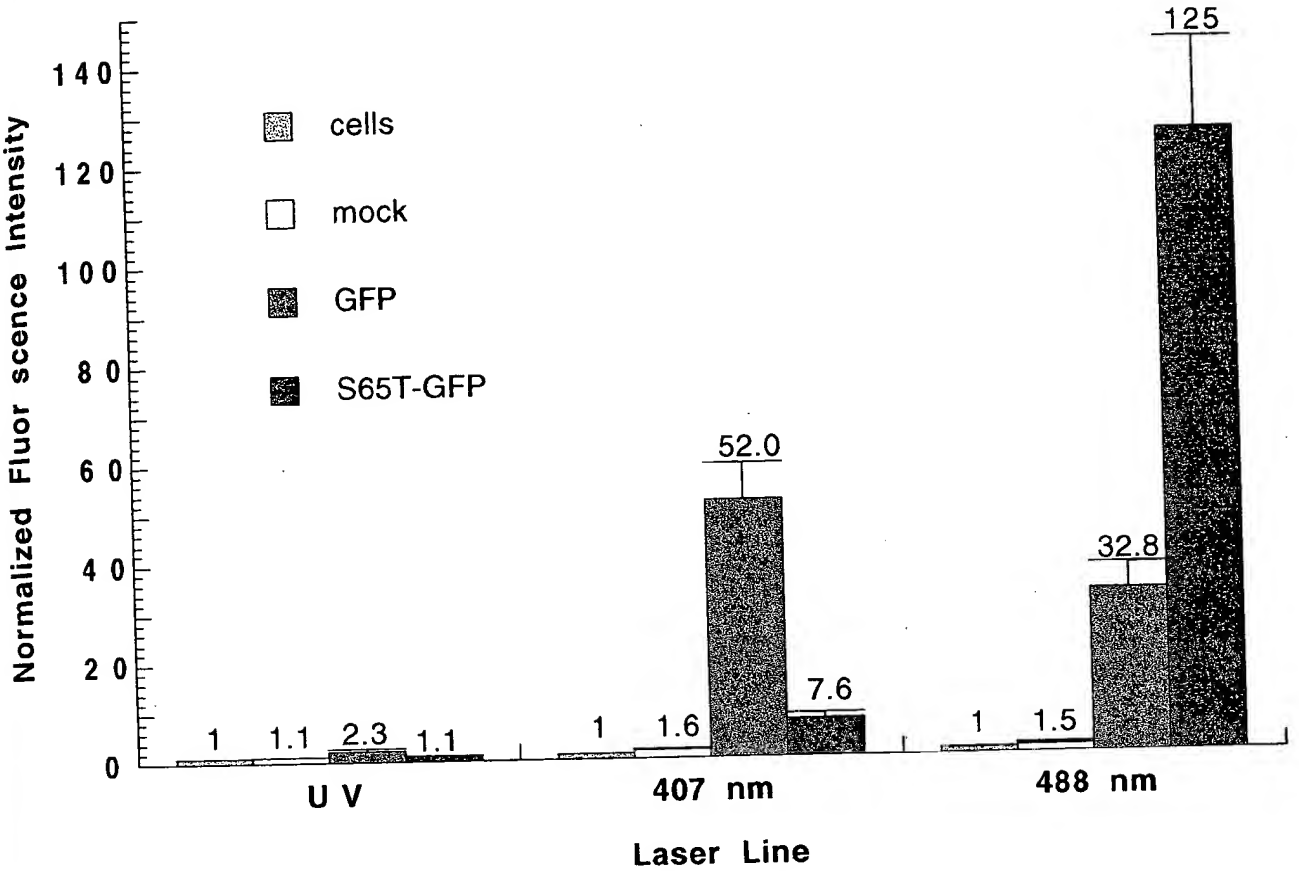


FIG. 5. Fluorescence intensity of sorted wt-GFP- and S65T-GFP-expressing cells relative to control pCMV mock-transfected or nontransfected cells as a function of laser wavelength. The linear fluorescence values were normalized such that nontransfected 293 cells emitted at one unit for each laser excitation wavelength. The plotted values and error bars represent normalized mean fluorescence and standard errors of the mean, respectively. For 488 and 407 nm, values are an average of four experiments for wt-GFP and five experiments for S65T-GFP, whereas the data for UV (351–355 nm) were obtained from three and two experiments, respectively, for wt- and S65T-GFP. A significantly higher mean fluorescence was observed for wt-GFP at 407 nm relative to 488 nm ($P = 0.0004$). In contrast, a significantly elevated fluorescence was found for S65T-GFP following excitation at 488 nm relative to 407 nm ($P < 0.0001$). A significantly higher fluorescence intensity was observed for S65T-GFP at 488 nm, relative to wt-GFP at 407 nm ($P < 0.0001$).

Heim et al. (8) that due to its increased brightness at 488 nm excitation, this form of GFP would be superior to wt-GFP. Prior to our study, however, it was unknown what level of cellular fluorescence could be achieved by exciting wt-GFP with a wavelength closer to its major excitation maximum.

Based on the observed reduction in background autofluorescence and proximity to the major excitation peak of wt-GFP (395 nm), we hypothesized that the 407 nm laser line could prove to be a more useful wavelength for wt-GFP analysis, compared with the more routinely available 488 nm excitation. Although green fluorescence can be detected following 488 nm excitation, the protein's absorbance spectrum suggests that this is a suboptimal excitation wavelength (18, 20, 29). Increased sensitivity of wt-GFP expression was observed by excitation at 407 nm; however, the intensity was still far below that from 488 nm excitation of S65T-GFP.

A practical advantage of monitoring S65T-GFP rather than wt-GFP at 488 nm is shown by the statistically significant difference in the percentage of cells with detectable S65T-GFP expression (50%) relative to wt-GFP expression (27%) by flow cytometric analysis. We believe these differences to be due to the increased fluorescence intensity of S65T-GFP relative to wt-GFP at this excitation wavelength. It is unlikely that these significant differences were due to variation in transfection efficiency as we have demonstrated that similar levels of GFP protein are present in wt-GFP- and S65T-GFP-transfected cells (Fig. 2). This observation is consistent with our assumption that similar transfection efficiencies were obtained by using the same transfection conditions for all vector constructs. It is worth noting that the only difference between the pCMV.gfp and the pCMV.S65T-gfp expression plasmids is the single nucleotide change for the S65T mutation and two silent nucleotide changes to generate a unique *Bst*EII site. The parental plasmid, including the promoter and all other regulatory elements, is identical to the wt-GFP- and S65T-GFP-expressing constructs.

A more likely explanation for the consistent differ-

ences observed in the percentage of cells with detectable expression between the pCMV.gfp and pCMV.S65T-gfp transfections is the inability to discriminate low level wt-GFP expression from non-expressing cells using 488 nm excitation. There is a clear nadir present between non-expressing and expressing cells in the S65T-GFP presort histogram which is not present in the corresponding histogram for wt-GFP (Fig. 4A). This significantly impedes our ability to gate wt-GFP-expressing cells precisely. Furthermore, we have observed that by altering transfection conditions using pCMV.gfp (i.e., increasing the amount of DNA added), it is possible to generate transfected populations with a higher percentage of cells possessing detectable expression, but without the corresponding high range of fluorescence intensity and nadir observed with S65T-GFP.

As evident from this example, the ability to detect specific fluorescence is directly related to the background cellular autofluorescence. Our data indicate significant variation in the magnitude of cellular autofluorescence when comparing 355, 407, and 488 nm excitation. Previous data suggest that pyridine nucleotides (e.g., NADH) are major contributers to blue autofluorescence following UV excitation (1, 25, 26), whereas flavin nucleotides and flavoproteins contribute green autofluorescence with 488 nm and UV excitation (1, 26). Our observation of a marked reduction in blue autofluorescence at 407 nm relative to UV is consistent with previous solution studies which indicate that the NADH absorption maximum (~365 nm) is closely approximated by the conventional UV excitation available from the argon ion laser, while absorption drops to near baseline levels with 407 nm excitation (1, 26). These same reports also suggest that riboflavin absorption is lower at 407 nm than at 488 nm, a finding which may explain our observation of a significantly reduced autofluorescence at 407 nm relative to 488 nm in 293 cells. The reduction in autofluorescence at 407 nm relative to both 488 nm and UV may provide part of the explanation for the improvement in wt-GFP detection at this wavelength. Aside from its utility for monitoring wt-GFP expression, our preliminary results (manuscript in preparation) further suggest that, due to lower autofluorescence, 407 nm may have advantages over UV excitation for immunofluorescence measurements in combination with a cascade blue-conjugated molecule.

The advantages of using 488 nm excitation to achieve increased sensitivity of detection with S65T-GFP rather than wt-GFP can be practically realized in many applications. Our report focused on flow cytometry and spectrofluorometry, but these results should extend to virtually any instrumentation which utilizes fluorescein-based detection.

## ACKNOWLEDGMENTS

The authors thank Linda DeYoung for assistance with spectrofluorometry, Jeanne Kahn for plasmid preparations, Meg Gordon for generating preliminary data demonstrating wt-GFP expression in 293 cells, David Giltinan and Ellen Gilkerson for assistance in statistical analysis and Mark Vasser and Peter Ng for oligonucleotide synthesis and purification. We additionally express our thanks to Samir Mittra and colleagues at Coherent, Inc., for making the model 302 laser available to us for these studies.

## LITERATURE CITED

1. Aubin JE: Autofluorescence of viable cultured mammalian cells. J Histochem Cytochemistry 27:36–43, 1979.
2. Bian J, Lin X, Tang J: Nuclear translocation of HIV-1 matrix protein p17: The use of *Aequorea victoria* green fluorescent protein in protein tagging and tracing. FASEB J 9:A1279, 1995.
3. Chalfie M, Tu Y, Euskirchen G, Ward WW, Prasher DC: Green fluorescent protein as a marker for gene expression. Science 263:802–805, 1994.
4. Cody CW, Prasher DC, Westler WM, Prendergast FG, Ward WW: Chemical structure of the hexapeptide chromophore of the Aequorea green-fluorescent protein. Biochemistry 32:1212–1218, 1993.
5. Cormier MJ, Hori K, Karkhanis YD, Anderson JM, Wampler JE, Morin JG, Hastings JW: Evidence for similar biochemical requirements for bioluminescence among the coelenterates. J Cell Physiol 81:291–297, 1973.
6. Delagrave S, Hawtin RE, Silva CM, Yang MM, Youvan DC: Red-shifted excitation mutants of the green fluorescent protein. Bio/Technology 13:151–154, 1995.
7. Flach J, Bossie M, Vogel J, Corbett A, Jinks T, Willins DA, Silver PA: A yeast RNA-binding protein shuttles between the nucleus and the cytoplasm. Mol Cell Biol 14:8399–8407, 1994.
8. Heim R, Cubitt AB, Tsien RY: Improved green fluorescence (letter). Nature 373:663–664, 1995.
9. Heim R, Prasher DC, Tsien RY: Wavelength mutations and posttranslational autoxidation of green fluorescent protein. Proc Natl Acad Sci USA 91:12501–12504, 1994.
10. Inouye S, Tsuji FI: Aequorea green fluorescent protein. Expression of the gene and fluorescence characteristics of the recombinant protein. FEBS Lett 341:277–280, 1994.
11. Johnson FH: Bioluminescence. In: Comprehensive Biochemistry. Vol. 27. Florkin M, Stotz EH (eds). Elsevier Publishing Co., Amsterdam, 1967.
12. Johnson FH, Shimomura O, Saiga Y, Gershman LC, Reynolds GT, Waters JR: Quantum efficiency of *Cypridina* luminescence, with a note on that of *Aequorea*. J Cell Comp Physiol 60:85–103, 1962.
13. Laemmli UK: Cleavage of structural proteins during the assembly of the head of bacteriophage T4. Nature 227:680–685, 1970.
14. Loken MR, Herzenberg LA: The analysis of cell populations with a fluorescence activated cell sorter. Ann NY Acad Sci 254:163–171, 1975.
15. Marshall J, Molloy R, Moss GW, Howe JR, Hughes TE: The jellyfish green fluorescent protein: A new tool for studying ion channel expression and function. Neuron 14:211–215, 1995.
16. Moores SL, Sabry JH, Spudich JA: Myosin dynamics in live Dictyostelium cells. Proc Natl Acad Sci USA, 1996, (in press).
17. Morin JG, Hastings JW: Biochemistry of the bioluminescence of colonial hydroids and other coelenterates. J Cell Physiol 77:305–312, 1971.
18. Morin JG, Hastings JW: Energy transfer in a bioluminescent system. J Cell Physiol 77:313–318, 1971.
19. Morin JG, Reynolds GT: Luminescence and related fluorescence in coelenterates. Biol Bull 139:430–431, 1970.
20. Morise H, Shimomura O, Johnson FH, Winant J: Intermolecular energy transfer in the bioluminescent system of Aequorea. Biochemistry 13:2656–2662, 1974.
21. Olmstead JB, Olson KR, McIntosh JR: Green fluorescent protein (GFP) chimeras as reporters for MAP 4 behavior in living cells. Mol Biol Cell 5:167a, 1994.
22. Prasher DC, Eckenrode VK, Ward WW, Prendergast FG, Cormier MJ: Primary structure of the Aequorea victoria green-fluorescent protein. Gene 111:229–233, 1992.
23. Samb Manu NY, 1
24. Shap Inc.,
25. Thor cenc chrc
26. Tho tane

23. Sambrook J, Fritsch EF, Maniatis T: Molecular Cloning: A Laboratory Manual. Cold Spring Harbor Laboratory Press, Cold Spring Harbor, NY, 1989.
24. Shapiro HM: Practical Flow Cytometry, Ed. 3. John Wiley and Sons, Inc., New York, 1995.
25. Thorell B: Flow cytometric analysis of cellular endogenous fluorescence simultaneously with emission from exogenous fluorochromes, light scatter and absorption. Cytometry 2:39–43, 1981.
26. Thorell B: Flow cytometric monitoring of intracellular flavins simultaneously with NAD(P)H levels. Cytometry 4:61–65, 1983.
27. Towbin H, Staehelin T, Gordon J: Electrophoretic transfer of proteins from polyacrylamide gels to nitrocellulose sheets: Procedure and some applications. Proc Natl Acad Sci USA 76:4350–4354, 1979.
28. Wang S, Hazelrigg T: Implications for bcd mRNA localization from spatial distribution of exu protein in Drosophila oogenesis. Nature 369:400–403, 1994.
29. Ward WW, Cody CW, Hart RC, Cormier MJ: Spectrophotometric identity of the energy-transfer chromophores in *Renilla* and *Aequorea* green-fluorescent proteins. Photochem Photobiol 31:611–615, 1980.

**STIC-ILL**

mic
QP501.F4
Adams

**From:** Canella, Karen
**Sent:** Thursday, January 09, 2003 6:41 PM
**To:** STIC-ILL
**Subject:** ill order 09/872,364

Art Unit 1642 Location 8E12(mail)

Telephone Number 308-8362

Application Number 09/872,364

1. FEBS Lett:
   1994, 351(2):211-214
   ~~1994, 341(2-3):277-280~~
2. Biochemistry, 1993, Vol. 32, pp. 1212-1218
3. PNAS, 1994, Vol. 91, pp. 12501-12504
4. Gene:
   1992, Vol. 111, pp. 229-233
   1996, Vol. 173, pp. 33-38
5. Cytometry, 1995 Dec 1, 21(4):309-317
6. Focus, 1996, 18(2):40-43

FEBS Letters 351 (1994) 211–214

FEBS 14472

# Evidence for redox forms of the *Aequorea* green fluorescent protein

Satoshi Inouye**, Frederick I. Tsuji*

*Marine Biology Research Division 0202, Scripps Institution of Oceanography, University of California at San Diego, La Jolla, CA 92093, USA*

Received 6 June 1994

**Abstract** Highly purified recombinant *Aequorea* green fluorescent protein is able to undergo a reversible oxidation-reduction reaction in the presence of molecular oxygen. In the oxidized form in near UV light, the protein is highly fluorescent, but when reduced with sodium dithionite, it becomes completely non-fluorescent. On exposure to molecular oxygen the reduced, non-fluorescent protein reverts to its original fluorescent state.

*Key words:* Oxidation–reduction; Electron transfer; Protein chromophore; Energy transfer; Bioluminescence; Aequorin

## 1. Introduction

The characteristic greenish bioluminescence of the jellyfish, *Aequorea victoria*, clearly visible as a ring of bright light along the margin of the umbrella [1], is due to the action of two closely associated proteins: aequorin, a small $Ca^{2+}$-binding protein (21.4 kDa) [2–4], and a green fluorescent protein (GFP, 27 kDa, fluorescence $\lambda_{max}$ = 508 nm) [5–9]. The latter contains a chromophore that is the ultimate emitter in the bioluminescence reaction [8,10]. Aequorin is made up of a complex of apoaequorin (apoprotein), coelenterazine (an imidazole compound, mol.wt. = 423) and molecular oxygen. When aequorin is mixed in vitro with $Ca^{2+}$, a bluish light is observed due to an intramolecular reaction in which the coelenterazine substrate is oxidized to coelenteramide. The reaction is catalyzed by the protein, which is converted to a luciferase on the binding of $Ca^{2+}$. The products are light ($\lambda_{max}$ = 470 nm), $CO_2$ and a blue fluorescent protein (BFP, coelenteramide + apoaequorin, fluorescence $\lambda_{max}$ = 470 nm). The electronically excited state of BFP (coelenteramide) is the emitter in the reaction. If the reaction is carried out in the presence of excess GFP, a greenish luminescence is observed, identical to that seen in the living animal. The greenish luminescence results from an energy transfer from the excited state of BFP to GFP [6,11,12].

$$\text{Aequorin} \xrightarrow{Ca^{2+}} \text{Blue fluorescent protein} + h\nu_{\lambda_{max}\,470\,nm} + CO_2$$
$$\downarrow + \text{GFP}$$
$$h\nu_{\lambda_{max}\,508\,nm}$$

We previously reported on the PCR cloning, expression, fluorescence characteristics, and energy transfer capability of *Aequorea* GFP [13]. The results showed that the properties of recombinant GFP are similar, if not identical, to those of native GFP. A further investigation of this recombinant protein has now revealed that it may exist in either an oxidized or reduced form. This finding and the key role that the protein plays in *Aequorea* bioluminescence have prompted us to examine the previous PCR-generated cDNA clone, since errors are known to occur in PCR cloning and because variation in nucleotide sequence has been reported for the cDNA for GFP [14]. Thus, the *Aequorea* cDNA library was re-screened, additional cDNA clones isolated, the DNA analyzed and the cDNA expressed in *E. coli* to prepare high purity recombinant GFP for characterization studies. This paper reports on this work and the redox properties of the purified recombinant GFP.

## 2. Materials and Methods

### 2.1. Materials

The following were obtained from commercial sources: Chelating Sepharose-Fast Flow, Pharmacia-LKB, Piscataway, NJ; imidazole, sodium dithionite ($Na_2S_2O_4$, 84% purity), $FeSO_4$, $K_4Fe(CN)_6$, $NaHSO_3$, $NaN_3$, NaCN, EDTA, L-cysteine, glutathione (reduced), dithiothreitol, 2-mercaptoethanol, 5,5′-dithio-bis-(2-nitrobenzoic acid) (DTNB), Sigma, St. Louis, MO; $NiCl_2$, Merck; hydrogen peroxide, platinum asbestos (5%), Fisher Scientific, Pittsburgh, PA; 2,2′-azino-di-(3-ethylbenzthiazoline-6-sulphonic acid) (ABTS), Calbiochem. San Diego, CA; sodium borohydride, Aldrich, Milwaukee, WI; bovine enterokinase (EK3), Biozyme, San Diego, CA; and SDS-PAGE gel and sample buffer, Novex, San Diego, CA.

### 2.2. Cloning of cDNA for GFP

The *Aequorea* cDNA library was screened using the *Bam*HI/*Sal*I insert of pAGP [13] as a probe. Subsequent isolation and sequence analysis of the cDNA clones for GFP were carried out as previously described [15].

### 2.3. Purification of rGFP

The *E. coli* expression system for the histidine-tagged GFP (His-GFP) and the procedure for purifying the expressed protein using a Ni-chelate affinity column were described previously [13]. The protein was eluted from the column using a linear gradient of imidazole (0–0.3 M). The fractions showing green fluorescence under near UV light (Model UVL-56, Ultraviolet Products, San Gabriel, CA) were collected and combined. The yield of this His-GFP was 1.3 mg from 300 ml of the cultured cells and the purity was greater than 95% as determined by SDS-polyacrylamide gel electrophoresis (SDS-PAGE). The fused region of His-GFP was removed by incubating 200 μg of the protein with 185 units (1 μg protein) of enterokinase in 1 ml of 50 mM sodium phosphate buffer, pH 6.0, at room temperature (22–24 °C) for 24 h. An aliquot of this digest was analyzed by SDS-PAGE and the remainder was dialyzed against 100 mM ammonium bicarbonate, pH 8.0. The dialysate was then applied to a freshly prepared Ni-chelate column (500 μl of gel bed) equilibrated with the same buffer and the pass-through fractions showing a green fluorescence (rGFP or His-GFP lacking the histidine tail) were collected and combined.

### 2.4. Protein analysis

Protein concentration was determined by the dye-binding method of Bradford [16] using a commercially available kit (Bio-Rad, Richmond, CA) and bovine serum albumin as a standard. SDS-PAGE was carried out under non-reducing conditions using a 8–16% separation gel according to Laemmli [17]. The rGFP in the enterokinase digest mixture

*Corresponding author. Fax: (1) (619) 534 7313.

**On leave from the Yokohama Research Center, Chisso Corp., Kanazawa-ku, Yokohama, Kanagawa 236, Japan.


*SSDI* 0014-5793(94)00859-0

was further purified by reversed-phase HPLC and then subjected to N-terminal amino acid sequence analysis using an Applied Biosystems (Foster City, CA) Model 470A gas phase protein sequencer connected to an on-line Model 120A phenylthiohydantoin analytical system.

*2.5. Reactions of rGFP with various chemical reagents*

The reactions of rGFP with various chemical reagents were carried out at room temperature in a final volume of 0.5 ml. The reaction was started by adding the chemical dissolved in 1 M ammonium bicarbonate, pH 8.0, to 20 μg of rGFP dissolved in 100 mM ammonium bicarbonate, pH 8.0. A transilluminator (Fischer Scientific, Model FBTIV-88) was used as a source of short UV light (312 nm) to monitor changes in the green fluorescence of the solution. In the reduction experiments with $NaBH_4$ and $H_2$/Pt, 100 μg of rGFP was used.

*2.6. Measurements of absorption and fluorescent spectra*

Absorption spectra of the purified rGFP were measured at room temperature with a Beckman Model DU-50 recording spectrophotometer and the fluorescence emission spectrum was measured with a Perkin-Elmer (Norwalk, CT) MPF-4 Fluorescence Spectrophotometer.

## 3. Results and discussion

In the previous study [13], two full-length cDNA clones for GFP were isolated by PCR and were found to have identical DNA sequences. In the present study, five positive clones, designated pAGP11, pAGP21, pAGP31, pAGP51 and pAGP71, were obtained from $1.5 \times 10^5$ clones. Sequence analysis [18] of pAGP11 and pAGP31 showed that they contained the full-length cDNA of GFP [13] and identical DNA sequences, including the 5′- and 3′-non-coding regions. The other clones, pAGP21, pAGP51 and pAGP71, were truncated forms of the 5′-coding region of GFP cDNA, which have been reported previously in pAGP [13] and *gfp*10 [14]. Thus, our studies have shown only one complete nucleotide sequence for GFP (Fig. 1) and the same primary structure, deduced from the nucleotide sequence, as reported previously [13].

Fig. 2A shows the N-terminal region of the fused His-GFP and the cleavage site of enterokinase. The expressed His-GFP was purified by Ni-chelate affinity chromatography and the histidine segment removed by treatment with enterokinase. After purification by HPLC, N-terminal amino acids sequence analysis yielded two sequences: DRWIPKM$^{I}$SKG, accounting for 40% of rGFP, and WIPKM$^{I}$SKGEE, accounting for the remaining 60% (Fig. 2A). The first sequence indicates that the fused region was cleaved correctly [19], but the reason for the two cleavages is unknown, unless the enterokinase has two cleavage sites instead of one or a contaminating protease is present. SDS-PAGE of His-GFP, carried out under non-reducing conditions with heat treatment, gave an apparent molecular mass of 31 kDa (Fig. 2B, lane l), whereas after cleavage with enterokinase the protein (rGFP) had an apparent molecular mass of 28 kDa (Fig. 2B, lane 2). An enterokinase band was not detected due to its low concentration. The calculated molecular weight of rGFP with 244 amino acid residues was 27,692.89. SDS-PAGE performed on rGFP under non-reducing conditions without heat treatment gave a greenish fluorescent band with an apparent molecular mass of about 40 kDa. While this band has been previously attributed to a partially denatured dimer [13], the true state of GFP in this band is unknown and it is also possible that the band is due to a monomer with an unusual electrophoretic mobility.

Fig. 3a shows the absorption spectrum of rGFP with peaks at 280, 395 and 478 nm. The spectrum was identical to that reported previously for native GFP [9]. His-GFP also gave the same absorption spectrum (data not shown). The fluorescence emission spectrum of rGFP (Fig. 3b) was virtually identical to

```
                                                                (EcoRI/NotI)tactacacacgaataaaagacaacaaag   -1

 M   S   K   G   E   E   L   F   T   G   V   V   P   I   L   V   E   L   D   G   D   V   N    23
atg agt aaa gga gaa gaa ctt ttc act gga gtt gtc cca att ctt gtt gaa tta gat ggc gat gtt aat    69

 G   Q   K   F   S   V   S   G   E   G   E   G   D   A   T   Y   G   K   L   T   L   K   F    46
ggg caa aaa ttc tct gtc agt gga gag ggt gaa ggt gat gca aca tac gga aaa ctt acc ctt aaa ttt   138

 I   C   T   T   G   K   L   P   V   P   W   P   T   L   V   T   T   F   S   Y   G   V   Q    69
att tgc act act ggg aag cta cct gtt cca tgg cca aca ctt gtc act act ttc tct tat ggt gtt caa   207

 C   F   S   R   Y   P   D   H   M   K   Q   H   D   F   F   K   S   A   M   P   E   G   Y    92
tgc ttt tca aga tac cca gat cat atg aaa cag cat gac ttt ttc aag agt gcc atg ccc gaa ggt tat   276

 V   Q   E   R   T   I   F   Y   K   D   D   G   N   Y   K   T   R   A   E   V   K   F   E   115
gta cag gaa aga act ata ttt tac aaa gat gac ggg aac tac aag aca cgt gct gaa gtc aag ttt gaa   345

 G   D   T   L   V   N   R   I   E   L   K   G   I   D   F   K   E   D   G   N   I   L   G   138
ggt gat acc ctt gtt aat aga atc gag tta aaa ggt att gat ttt aaa gaa gat gga aac att ctt gga   414

 H   K   M   E   Y   N   Y   N   S   H   N   V   Y   I   M   A   D   K   P   K   N   G   I   161
cac aaa atg gaa tac aac tat aac tca cat aat gta tac atc atg gca gac aaa cca aag aat gga atc   483

 K   V   N   F   K   I   R   H   N   I   K   D   G   S   V   Q   L   A   D   H   Y   Q   Q   184
aaa gtt aac ttc aaa att aga cac aac att aaa gat gga agc gtt caa tta gca gac cat tat caa caa   552

 N   T   P   I   G   D   G   P   V   L   L   P   D   N   H   Y   L   S   T   Q   S   A   L   207
aat act cca att ggc gat ggc cct gtc ctt tta cca gac aac cat tac ctg tcc aca caa tct gcc ctt   621

 S   K   D   P   N   E   K   R   D   H   M   I   L   L   E   F   V   T   A   A   G   I   T   230
tcc aaa gat ccc aac gaa aag aga gat cac atg atc ctt ctt gag ttt gta aca gct gct ggg att aca   690

 H   G   M   D   E   L   Y   K   *                                                           238
cat ggc atg gat gaa cta tac aaa taa atgtccagacttccaattgacactaaagtgtccgaacaattactaaattctcagg   797

gttcctggttaaattcaggctgagactttatttatatatttatagattcattaaaatttttatgaataatttattgatgttattaatagggg   888
ctattttcttattaaataggctactggagtgtat(NotI/EcoRI)                                              922
```

Fig. 1. Nucleotide sequence of *Aequorea* GFP and primary structure of GFP deduced from the nucleotide sequence. The hexapeptide segement involved in the cyclic formation of the fluorescent chromophore is underlined [8,10,21]. GenBank Accession Number is L29345.

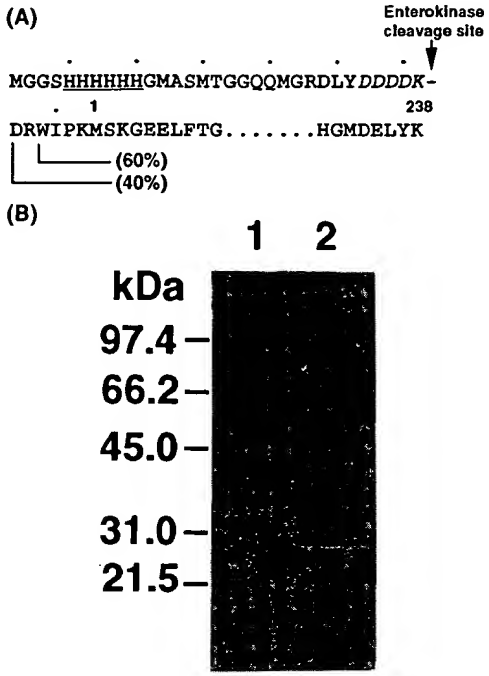


Fig. 2. N-Terminal amino acid sequence and SDS-PAGE of His-GFP. (A) N-Terminal amino acid sequence showing the 34 amino acid residues plus the 3 amino acid residues arising from use of the PCR primer, with the 6 histidine residues underlined and the enterokinase cleavage site indicated by an arrow. (B) SDS-PAGE of His-GFP before (lane 1: 5 $\mu$g of protein applied) and after (lane 2: 4 $\mu$g of protein applied) cleavage with enterokinase. Molecular weight markers (Bio-Rad): phosphorylase b (97,400), bovine serum albumin (66,200), ovalbumin (45,000), carbonic anhydrase (31,000), and soybean trypsin inhibitor (21,500).

those reported previously for native GFP [9] and for His-GFP [13] and the fluorescence excitation spectrum (read at $\lambda$ = 530 nm) gave peaks at 395 and 478 nm, closely matching the peaks of the absorption spectrum. However, the ratios of the absorbance peaks, 395 nm/280 nm, for rGFP and His-GFP were 0.43 and 0.40, respectively, which are approximately one-half of the value reported for native GFP [8,10]. The difference in the ratios is presumably due to the presence of a second tryptophan in the fused N-terminus of each of the proteins (Fig. 2A).

The expressed GFP in near UV light has been found to show strong intrinsic fluorescence, both intracellularly and extracellularly [13,20]. The fluorescence has been attributed to the presence of a chromophore in the protein, formed by the cyclization of three amino acid residues within an hexapeptide segment of the polypeptide chain by post-translational modification [8,10]. Considerable work has gone into the chemical structure of the chromophore [8,10,21], but the chemical basis for the fluorescence is still unknown. During the purification of His-GFP, a marked increase in fluorescence intensity was observed when the harvested cells and cell-precipitate were allowed to stand overnight at room temperature. Subsequently, the intensity remained unchanged for over a month. This suggested that an oxidative step may be involved in the initial increase in fluorescence.

On adding sodium dithionite ($Na_2S_2O_4$), a strong reducing reagent, to a solution of rGFP, the green fluorescence of the solution disappeared within a few minutes and, on standing for several hours, the fluorescence reappeared first as a thin band at the surface, which then spread slowly downward into the solution. On standing overnight the solution recovered its fluorescence completely. This result indicated that the rGFP was involved in a redox reaction with molecular oxygen, with the oxidized form being fluorescent and the reduced form being nonfluorescent.

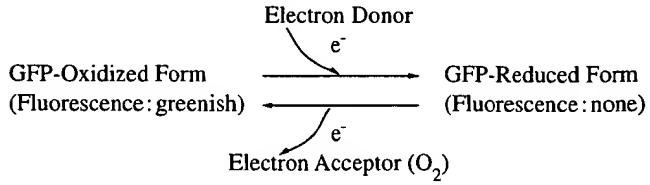


Table 1 summarizes the results of mixing various chemical reagents (reductants and oxidants) with rGFP. Some of the compounds were examined under both aerobic and anaerobic conditions, as noted in the table. The addition of either $FeSO_4$ or ABTS [22], to a solution of rGFP under argon atmosphere caused the greenish fluorescence to be quickly extinguished and, as with $Na_2S_2O_4$, the reaction was reversible, that is, on standing in air the greenish fluorescence returned once more. However, when rGFP was treated with $Na_2S_2O_4$, $FeSO_4$ or ABTS in an argon atmosphere and allowed to stand, the greenish fluorescence did not return until air was readmitted. The time required for the recovery of the greenish fluorescence was shortened if the solution was shaken in air or subjected to dialysis. In order to ascertain whether any spectral change occurs on reduction, 450 $\mu$l of a 0.18 mg/ml solution of rGFP in 50 mM ammonium bicarbonate, pH 8.0, was mixed with 25 $\mu$l of 100 mM sodium dithionite in 1 M ammonium bicarbonate, pH 8.0, and the mixture was scanned between 600 and 300 nm in a microcell using an Uvikon 810 (Kontron, Zurich, Switzerland) recording spectrophotometer. Controls consisted of (a) 450 $\mu$l of the same rGFP solution mixed with 25 $\mu$l of the

Table 1
Reactions of various chemical reagents with rGFP

| Addition to rGFP | Green fluorescence | $E_0'$, V |
|---|---|---|
| None | (+) | |
| $Na_2S_2O_4$ (5 mM) | | |
| under $Ar_2$ | (+) → (−) | −0.66 |
| exposure to air/dialysis | (+) ← (−) | |
| $FeSO_4$ (2 mM) | | |
| under $Ar_2$ | (+) → (−) | 0.77 |
| exposure to air/dialysis | (+) ← (−) | |
| 1/2 $O_2$ + $2H^+/H_2O$ | | 0.82 |
| ABTS (0.2 mM) | | |
| under $Ar_2$ | (+) → (−) | |
| exposure to air/dialysis | (+) ← (−) | |
| $H_2O_2$ (1%) under $Ar_2$ or Air | (+) → (−) | 0.30 |
| $H_2$/Pt (~1 mg) | (+) → (−) | −0.42 |
| $NaBH_4$ (~1 mg) under $Ar_2$ or Air | (+) | |
| 2-Mercaptoethanol (2%) | (+) | |
| Dithiothreitol (10 mM) | (+) | −0.33 |
| Glutathione, reduced (10 mM) | (+) | −0.23 |
| L-Cysteine (10 mM) | (+) | |
| $K_4Fe(CN)_6$ (2 mM) | (+) | 0.36 |
| $NaHSO_3$ (10 mM) | (+) | |
| $NaN_3$ (10 mM) | (+) | |
| NaCN (10 mM) | (+) | |
| EDTA (10 mM) | (+) | |

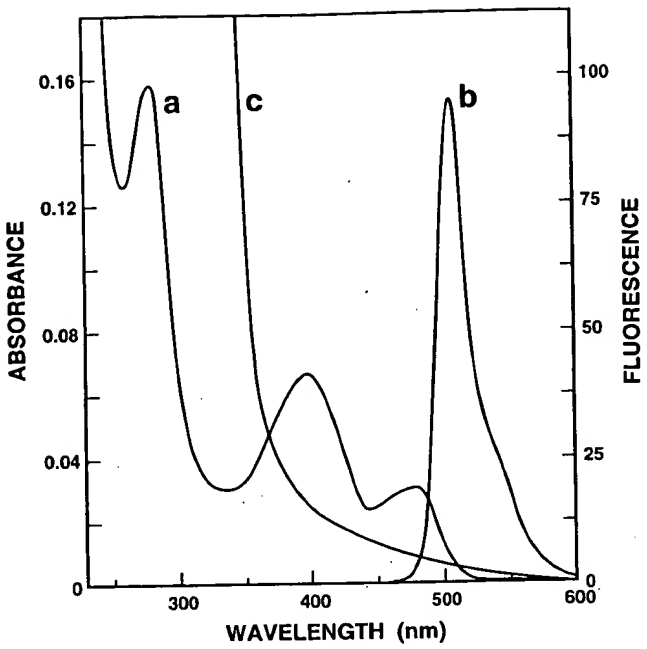


Fig. 3. Absorption and fluorescence emission spectra of rGFP. (a) Absorption spectrum of rGFP. (b) Fluorescence emission spectrum of rGFP. (c) Absorption spectrum of $H_2O_2$-treated rGFP. For (a), (b) and (c) the protein concentration was 0.18 mg/ml in 100 mM ammonium bicarbonate, pH 8.0.

same 1 M ammonium bicarbonate soution, and (b) 450 $\mu$l of the same 50 mM ammonium bicarbonate solution mixed with 25 $\mu$l of the same sodium dithionite solution. Except for the region between 400 and 300 nm, which was difficult to analyze due to the high absorbance of sodium dithionite, the absorption spectrum of the rGFP-sodium dithionite mixture did not show any major change in absorbance, shape or maximum ($\lambda_{max}$ = 478 nm) between 600 and 400 nm when compared to the oxidized rGFP control. Thus, between 600 and 400 nm there appears to be no apparent change in absorption spectrum on reduction. If hydrogen peroxide was added to rGFP, the green greenish fluorescence slowly disappeared over a period of 1 h and never recovered even when exposed to air. This loss of greenish fluorescence was accompanied by a disappearance of the absorbance peaks at 395 and 478 nm (Fig. 3c), suggesting that a permanent structural change had taken place in the chromophore. Since rGFP is reduced by $FeSO_4$ and the reduced rGFP oxidized by $O_2$, with $H_2O$ being a likely product, it appears that the standard reduction potential, $E'_o$, for rGFP lies somewhere between 0.77 V and 0.82 V (Table 1). Moreover, with the $E'_o$s for rGFP and $O_2$ lying so close to each other, it is conceivable that GFP may be at the terminus of a series of electron carriers, as in the eukaryotic respiratory chain.

The rGFP has two cysteine residues at positions 48 and 70 in the primary structure [13,14]. Reducing reagents such as 2-mercaptoethanol, dithiothreitol, reduced glutathione and L-cysteine did not have any affect on the fluorescence of rGFP (Table 1), whereas treatment with the sulfhyryl reagent DTNB (1 mM) [23] caused the greenish fluorescence to disappear in a few minutes (data not shown). Thus, a free cysteine residue may be required for the greenish fluorescence of rGFP.

It is noteworthy that reversible photobleaching of GFP has been reported in vivo on exposure to UV light during the expression of the cDNA for GFP in *Caenorhabditis elegans* [20]. It is possible that the photobleaching may be due to a reduction taking place within the cell and the recovery of fluorescence to the transfer of electrons to molecular oxygen. The proposed imidazolone structure for the chromophore of GFP [8,10,21], however, does not appear to explain the redox behavior of rGFP in that the electron acceptor–donor group is not identifiable. Another interesting structure-related problem is that *Aequorea* GFP, when expressed in such diverse organisms as *E. coli*, *C. elegans* and COS cells, is fluorescent [13,20]. This must mean that a synthetic (enzymatic) mechanism must be present in all of these organism to form the complex chromophore by post-translational modification or a self-modification mechanism must exist within the protein.

*Acknowledgements:* The authors are grateful to Drs. M. Shimonaka and Y. Yamaguchi for their assistance in the HPLC purification of rGFP and to Dr. G. Fortes for help with the fluorescence measurements. The research was supported in part by Research Grant MCB91-04684 from the National Science Foundation.

## References

[1] Harvey, E.N. (1952) Bioluminescence, Academic Press, New York.
[3] Inouye, S., Noguchi, M., Sakaki, Y., Takagi, Y., Miyata, T., Iwanaga, S., Miyata, T. and Tsuji, F.I. (1985) Proc. Natl. Acad. Sci. USA 82, 3154–3158.
[4] Charbonneau, H., Walsh, K.A., McCann, R.O., Prendergast, F.G., Cormier, M.J. and Vanaman, T.C. (1985) Biochemistry 24, 6762–6771.
[5] Shimomura, O., Johnson, F.H. and Saiga, Y. (1962) J. Cell. Comp. Physiol. 59, 223–239.
[6] Johnson, F.H., Shimomura, O., Saiga, Y., Gershman, L.C., Reynolds, G.T. and Waters, J.R. (1962) J. Cell. Comp. Physiol. 60, 85–103.
[7] Prendergast, F.G. and Mann, K.G. (1978) Biochemistry 17, 3448–3453.
[8] Shimomura, O. (1979) FEBS Lett. 104, 220–222.
[9] Ward, W.W., Cody, C.W., Hart, R.C. and Cormier, M.J. (1980) Photochem. Photobiol. 31, 611–615.
[10] Cody, C.W., Prasher, D.C., Westler, W.M., Prendergast, F.G. and Ward, W.W. (1993) Biochemistry 32, 1212–1218.
[11] Morin, J.G. and Hastings, J.W. (1971) J. Cell. Physiol. 77, 313–318.
[12] Morise, H., Shimomura, O., Johnson, F.H. and Winant, J. (1974) Biochemistry 13, 2656–2662.
[13] Inouye, S. and Tsuji, F.I. (1994) FEBS Lett. 341, 277–280.
[14] Prasher, D.C., Eckenrode, V.K., Ward, W.W., Prendergast, F.G. and Cormier, M.J. (1992) Gene 111, 229–233.
[15] Inouye, S. and Tsuji, F.I. (1993) FEBS Lett. 315, 343–346.
[16] Bradford, M.M. (1976) Anal. Biochem. 72, 248–254.
[18] Sanger, F., Nicklen, S. and Coulson, A.R. (1977) Proc. Natl. Acad. Sci. USA 74, 5463–5467.
[19] LaVallie, E.R., Rehemtulla, A., Racie, L.A., DiBlasio, E.A., Ferenz, C., Grant, K.L., Light, A. and McCoy, J.M. (1993) J. Biol. Chem. 268, 23311–23317.
[20] Chalfie, M., Tu, Y., Euskirchen, G., Ward, W.W. and Prasher, D.C. (1994) Science 263, 802–805.
[21] McCapra, F., Razavi, Z. and Neary, A.P. (1988) J. Chem. Soc. Chem. Commun. 790–791.
[22] Childs, R.E. and Bardsley, W.G. (1975) Biochem. J. 145, 93–103.
[23] Ellman, G.E. (1959) Arch. Biochem. Biophys. 82, 70–77.

**STIC-ILL**

**From:** Canella, Karen
**Sent:** Thursday, January 09, 2003 6:41 PM
**To:** STIC-ILL
**Subject:** ill order 09/872,364

Art Unit 1642 Location 8E12(mail)

Telephone Number 308-8362

Application Number 09/872,364

1. FEBS Lett:
   1994, 351(2):211-214
   1994, 341(2-3):277-280

2. Biochemistry, 1993, Vol. 32, pp. 1212-1218

3. PNAS, 1994, Vol. 91, pp. 12501-12504

4. Gene:
   1992, Vol. 111, pp. 229-233
   1996, Vol. 173, pp. 33-38

5. Cytometry, 1995 Dec 1, 21(4):309-317

6. Focus, 1996, 18(2):40-43

*Proc. Natl. Acad. Sci. USA*
Vol. 91, pp. 12501–12504, December 1994
Biochemistry

# Wavelength mutations and posttranslational autoxidation of green fluorescent protein

(*Aequorea victoria*/blue fluorescent protein/*Escherichia coli*/imidazolidinone)

ROGER HEIM*, DOUGLAS C. PRASHER†, AND ROGER Y. TSIEN*‡

*Howard Hughes Medical Institute, University of California, San Diego, La Jolla, CA 92093-0647; and †U.S. Dept. of Agriculture, Animal and Plant Health Inspection Service, Otis Methods Development Center, Otis Air National Guard Base, MA 02542

*Communicated by Eric R. Kandel, August 19, 1994*

ABSTRACT **The green fluorescent protein (GFP) of the jellyfish *Aequorea victoria* is an unusual protein with strong visible absorbance and fluorescence from a *p*-hydroxybenzylidene-imidazolidinone chromophore, which is generated by cyclization and oxidation of the protein's own Ser-Tyr-Gly sequence at positions 65–67. Cloning of the cDNA and heterologous expression of fluorescent protein in a wide variety of organisms indicate that this unique posttranslational modification must be either spontaneous or dependent only on ubiquitous enzymes and reactants. We report that formation of the final fluorophore requires molecular oxygen and proceeds with a time constant (≈4 hr at 22°C and atmospheric $pO_2$) independent of dilution, implying that the oxidation does not require enzymes or cofactors. GFP was mutagenized and screened for variants with altered spectra. The most striking mutant fluoresced blue and contained histidine in place of Tyr-66. The availability of two visibly distinct colors should significantly extend the usefulness of GFP in molecular and cell biology by enabling *in vivo* visualization of differential gene expression and protein localization and measurement of protein association by fluorescence resonance energy transfer.**

Proteins are often labeled with fluorescent tags to detect their localization and sometimes their conformational changes both *in vitro* and in intact cells. Such labeling is essential both for immunofluorescence and for fluorescence analog cytochemistry, in which the biochemistry and trafficking of proteins are monitored after microinjection into living cells (1). Traditionally, fluorescence labeling is done by purifying proteins and then covalently conjugating them to reactive derivatives of organic fluorophores. The stoichiometry and locations of dye attachment are often difficult to control, and careful repurification of the proteins is usually necessary. If the proteins are to be used inside living cells, a final challenging step is to get them across the plasma membrane via micropipet techniques or various methods of reversible permeabilization.

An alternative would be to devise molecular biological means to generate fluorescent proteins. The natural UV fluorescence of tryptophan residues is of little use except in the simplest *in vitro* samples, because the wavelengths are too short and tryptophan is too ubiquitous for any one protein to stand out in a complex biological mixture. A more promising strategy would be to concatenate the gene for the nonfluorescent protein of interest with the gene for a naturally fluorescent protein and express the fusion product. The most highly fluorescent proteins known are the phycobiliproteins (2), but their fluorescence depends entirely on correct enzymatic insertion of a difficult-to-obtain tetrabilin chromophore into a large apoprotein (3). The green fluorescent protein (GFP) from the jellyfish *Aequorea victoria* is a much smaller molecule of 238 amino acids, whose natural function seems to be to convert the blue chemiluminescence of the $Ca^{2+}$-sensitive photoprotein aequorin into green emission (4). GFP's absorption bands in the blue and emission peak in the green do not arise from a distinct cofactor but rather from an internal *p*-hydroxybenzylideneimidazolidinone chromophore generated by cyclization and oxidation of a Ser-Tyr-Gly sequence at residues 65–67 (5). When the gene for GFP was first cloned (6), whether jellyfish-specific enzymes were required for this posttranslational modification was unknown. Heterologous expression of the gene in *Escherichia coli* (7, 8), *Caenorhabditis elegans* (7), *Saccharomyces cerevisiae* (R.H., S. D. Emr and R.Y.T., unpublished data), and *Drosophila melanogaster* (9) showed that additional *Aequorea*-specific enzymes were not required because the protein became brightly fluorescent in all these organisms.

The ability to generate fluorescence *in situ* by expressing the gene for GFP has opened up tremendous possibilities for continuously monitoring gene expression, cell developmental fates, and protein trafficking in living, minimally perturbed cells, tissues, and organisms. Nevertheless, major questions about GFP itself remain. What is the mechanism of fluorophore formation? How does fluorescence relate to protein structure? Can its fluorescence properties be tailored and improved—in particular, to provide a second distinguishable color for comparison of independent proteins and gene expression events? This study provides initial answers.

## MATERIALS AND METHODS

The coding region of a clone of *A. victoria gfp10* cDNA (6) was amplified by the PCR (7) to create *Nde* I and *Bam*HI sites at the 5′ and 3′ ends, respectively, and cloned behind the T7 promoter of pGEMEX-2 (Promega), replacing most of the T7 gene *10*. The resulting plasmid was transformed into *E. coli* strain JM109(DE3), and high-level expression was achieved by growing the cultures at 24°C to saturation without induction by isopropyl β-D-thiogalactoside. Random mutagenesis of the *gfp* cDNA was done by hydroxylamine treatment (10) or by increasing the error rate of the PCR with 0.1 mM $MnCl_2$, 50 μM dATP, and 200 μM of dGTP, dCTP, and dTTP (11). The product was ligated into pGEMEX-2 and subsequently transformed into strain JM109(DE3). Colonies on agar were visually screened for different emission colors and ratios of brightness when excited at 475 vs. 395 nm, supplied by a xenon lamp and grating monochromator for which the output beam was expanded to illuminate an entire culture dish.

To prepare soluble extracts, cells from a 1.5-ml suspension were collected, washed, and resuspended in 150 μl of 50 mM Tris·HCl, pH 8.0/2 mM EDTA. Lysozyme and DNase I were added to 0.2 mg/ml and 20 μg/ml, respectively, and the samples were incubated on ice until lysis occurred (1–2 hr).

The publication costs of this article were defrayed in part by page charge payment. This article must therefore be hereby marked "*advertisement*" in accordance with 18 U.S.C. §1734 solely to indicate this fact.

Abbreviation: GFP, green fluorescent protein.

‡To whom reprint requests should be addressed.

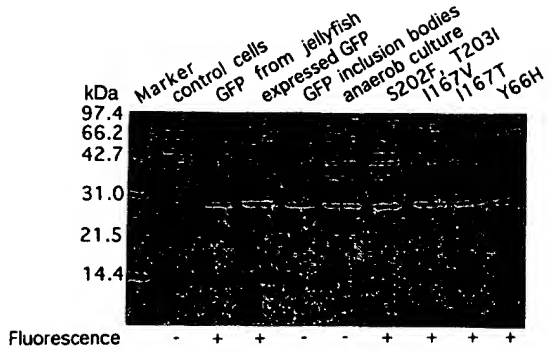


FIG. 1. GFP expression in *E. coli*: Variations in fluorescence properties despite equalized apoprotein contents. Different versions of GFP are compared by gel electrophoresis and Coomassie blue staining. Soluble extracts of *E. coli* expressing GFP show a predominant band that is absent in extracts from control cells and has the same electrophoretic mobility as native GFP isolated from the jellyfish *A. victoria* (5). Inclusion bodies of expressing cells consist mainly of nonfluorescent GFP, which has the same mobility as soluble GFP. Nonfluorescent soluble GFP of anaerobically grown (anerob) cultures is also a major band with correct mobility. Soluble extracts of the mutated clones H9 (S202F, T203I), P9 (I167V), P11 (I167T), and P4 (Y66H) again contain a dominant protein with essentially the same molecular mass.

The lysates were then clarified by centrifuging at 12,000 × *g* for 15 min. Anaerobic cultures were grown in GasPak pouches (Becton Dickinson). Inclusion bodies were obtained as described (12).

Excitation and emission spectra were measured with 1.8-nm bandwidths, and the nonscanning wavelength was set to the appropriate peak. Excitation spectra were corrected with a rhodamine B quantum counter, whereas emission spectra (except for mutation Y66W) were corrected for monochromator and detector efficiencies by using manufacturer-supplied correction spectra.

## RESULTS AND DISCUSSION

GFP was expressed in *E. coli* under the control of a T7 promoter for quantitative analysis of the properties of the recombinant protein. Gel electrophoresis under denaturing conditions showed protein of the expected molecular mass (27 kDa) as a dominant band (Fig. 1), which could be quantified simply by densitometry of staining with Coomassie blue. Soluble recombinant GFP proved to have identical spectra and the same or even slightly more fluorescence per mol of protein as GFP purified from *A. victoria*, showing that the soluble protein in *E. coli* undergoes correct folding and oxidative cyclization with as high an efficiency as in the jellyfish. The bacteria also contained inclusion bodies consisting of protein indistinguishable from jellyfish or soluble recombinant protein on denaturing gels (Fig. 1). However, this material was completely nonfluorescent, lacked the visible absorbance bands of the chromophore, and did not become fluorescent when solubilized and subjected to protocols that renature GFP (13). Therefore protein from inclusion bodies seemed unable to generate the internal chromophore.

An interesting intermediate stage in protein maturation could be generated by growing the bacteria anaerobically. The soluble protein again looked the same as GFP on denaturing gels (Fig. 1) but was nonfluorescent. In this case, fluorescence gradually developed after admission of air, even when fresh protein synthesis was blocked by using puromycin and tetracycline. Evidently the soluble nonfluorescent protein synthesized under anaerobic conditions was ready to become fluorescent once atmospheric oxygen was readmitted. The fluorescence per protein molecule approached its final asymptotic value with a single-exponential time course and a rate constant of $0.24 \pm 0.06\ hr^{-1}$ (at 22°C), measured either in intact cells with protein-synthesis inhibitors or in lysates in which the soluble proteins and cofactors were $\approx 10^5$ more dilute than in cells. Such pseudo-first-order kinetics strongly suggest that no enzymes or cofactors are necessary for the final step of fluorophore formation in GFP. A tentative molecular interpretation is presented in Fig. 2. If the newly translated apoprotein evades precipitation into inclusion bodies, the amino group of Gly-67 might cyclize onto the carbonyl group of Ser-65 to form an imidazolidin-5-one, where the process would stop were $O_2$ absent. The new N=C double bond would be expected to promote dehydrogenation to form a conjugated chromophore; imidazolidin-5-ones undergo autoxidative formation of double bonds at the 4-position (14, 15), which would complete the fluorophore (Fig. 2, upper right). Because fluorophore formation requires at least one step with a time constant of ≈4 hr, use of GFP as a reporter protein to monitor faster changes in promoter activity may be problematic.

A major question in protein photophysics is how a single chromophore can give widely different spectra depending on its local protein environment. This question has received the most attention with respect to the multiple colors of visual pigments based on retinal (16) but is also important in GFP. The GFP from *Aequorea* and that of the sea pansy *Renilla reniformis* share the same chromophore, yet *Aequorea* GFP

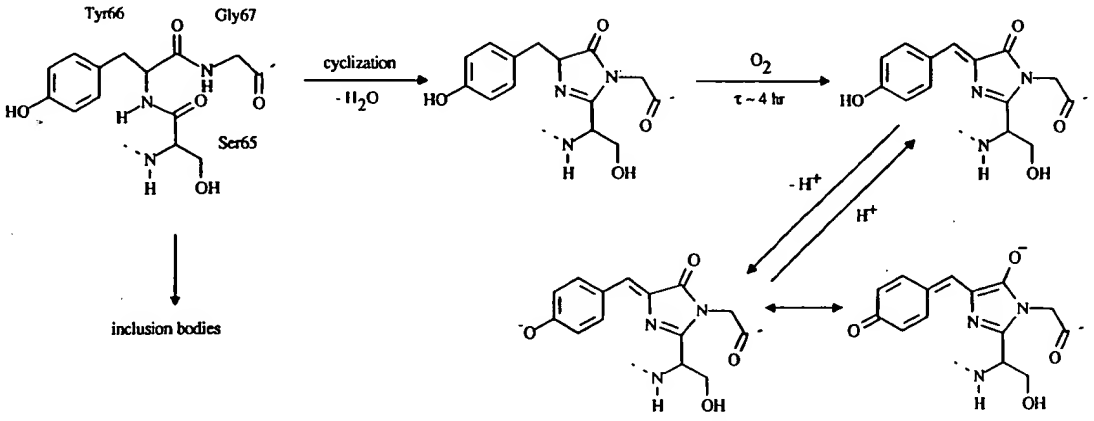


FIG. 2. Proposed biosynthetic scheme for the chromophore of GFP. The freshly translated protein (upper left) could be trapped by inclusion bodies or remain soluble and nonfluorescent (upper center) until oxidation by $O_2$, which would dehydrogenate Tyr-66 to form the fluorophore (upper right). The protonated and deprotonated species (upper and lower right) may be responsible for the 395- and 470- to 475-nm excitation peaks, respectively. The excited states of phenols are much more acidic than their ground states, so that emission would come only from the deprotonated species.

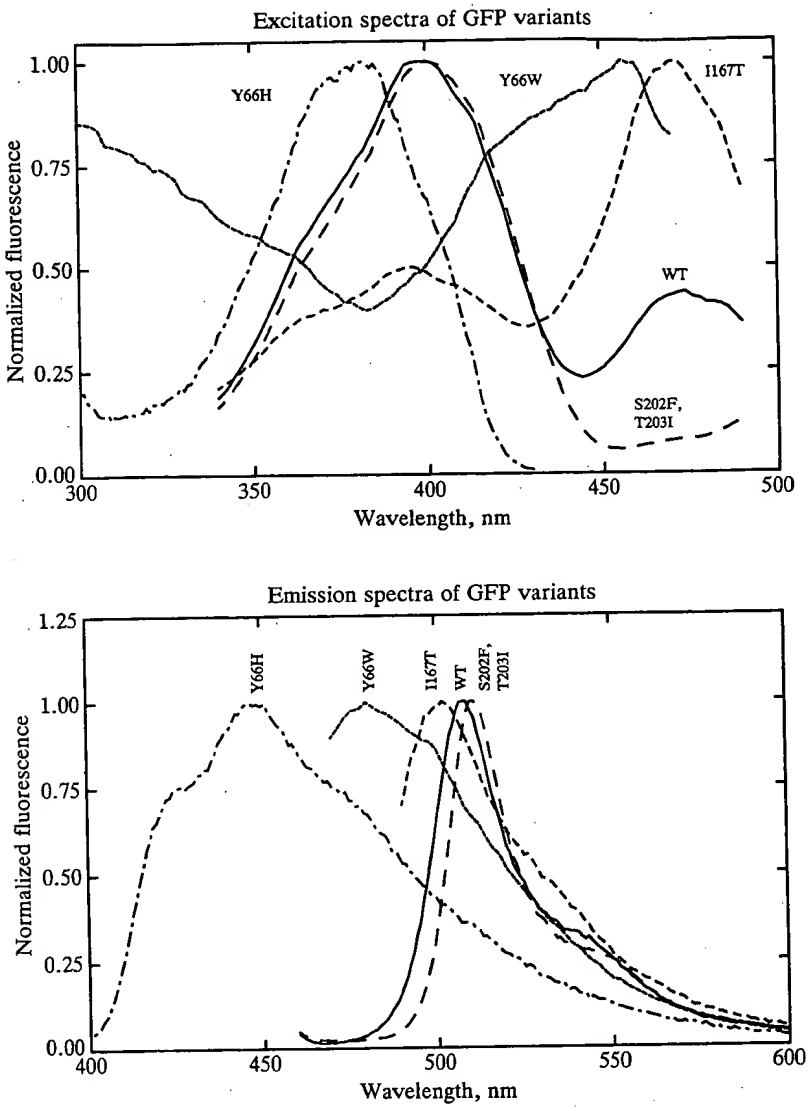


FIG. 3. Excitation and emission spectra of Wild-type and mutant GFPs. ——, Wild-type; — —, mutations S202F, T203I; – – –, mutation I167T; ------, mutation Y66W; —·—, mutation Y66H. Samples were soluble fractions from *E. coli* expressing the proteins at high level, except for mutant Y66W, which was obtained in very low yield and measured on intact cells. Autofluorescence was negligible for all spectra except those of mutant Y66W, whose excitation spectrum below 380 nm may be contaminated by autofluorescence. All amplitudes have been arbitrarily normalized to a maximum value of 1.0. To compare brightnesses at equal protein concentrations, see Table 1.

has two absorbance peaks at 395 and 475 nm, whereas *Renilla* GFP has only a single absorbance peak at 498 nm, with ≈5.5-fold greater monomer extinction coefficient than the major 395-nm peak of the *Aequorea* protein (17). The isolated chromophore and denatured protein at neutral pH do not match either native protein (5). For many practical applications, the spectrum of *Renilla* GFP would be preferable to that of *Aequorea* because wavelength discrimination between different fluorophores and detection of resonance energy transfer are easier when the component spectra are tall and narrow rather than low and broad. Furthermore, the longer wavelength excitation peak (475 nm) of *Aequorea* GFP is almost ideal for fluorescein filter sets and is resistant to photobleaching but has lower amplitude than the shorter wavelength peak at 395 nm, which is more susceptible to photobleaching (7). For all these reasons, it would be interesting to convert the *Aequorea* GFP excitation spectrum to a single peak, preferably at longer wavelengths. The cDNA was therefore subjected to random mutagenesis by hydroxylamine treatment or PCR. Approximately six thousand bacterial colonies on agar plates were illuminated with alternating 395- and 475-nm excitation and visually screened for altered excitation properties or emission colors. Although this number of colonies falls far short of saturating the possible mutations of a protein of 238 residues, interesting variants have already appeared. Three mutants were found with significant alterations in the ratio of the two main excitation peaks (Fig. 3 and Table 1). Compared with wild-type GFP, mutant H9 had increased fluorescence at 395-nm excitation, whereas mutants P9 and P11 were more fluorescent at 475-nm excitation, mutant P11 being the best species for fluorescein filters. The mutations were sequenced and recombined with the wild-type gene in different ways to eliminate neutral mutations and assign the fluorescence effects to single-amino acid substitutions (except for mutant H9, where two neighboring mutations have not yet been separated). The mutations all lay in the C-terminal part of the protein (Table 1), remote in primary sequence from the chromophore formed from residues 65–67. Determination of the three-dimensional structure of GFP should enable detailed interpretation of these spectral perturbations. One possibility is that the mutations at Ile-167 shift a positive charge slightly closer to the phenolic group of the fluorophore; this shift should both increase the percentage of phenolic anion, which is probably the species responsible for the 470- to 475-nm

Table 1. Characteristics of mutated vs. wild-type GFP

| GFP | Mutation | Excitation maxima,* nm | Emission maxima,† nm | Relative fluorescence,‡ % |
|---|---|---|---|---|
| Wild type | None | 396 (476) | 508 (503) | (=100) |
| Mutant H9 | Ser-202 → Phe, Thr-203 → Ile | 398 | 511 | 117§ |
| Mutant P9 | Ile-167 → Val | 471 (396) | 502 (507) | 166¶ |
| Mutant P11 | Ile-167 → Thr | 471 (396) | 502 (507) | 188¶ |
| Mutant P4 | Tyr-66 → His | 382 | 448 | 57‖ |
| Mutant W | Tyr-66 → Trp | 458 | 480 | ND |

*Values in parentheses are lower-amplitude peaks.
†Primary values were seen when exciting at the main excitation peak; values in parentheses were seen when illuminating at the lower-amplitude excitation peak.
‡Equal amounts of protein were used based on densitometry of gels stained with Coomassie blue (Fig. 1). ND, not done.
§Emission maxima of spectra recorded at excitation 395 nm were compared.
¶Emission maxima of spectra recorded at excitation 475 nm were compared.
‖Emission spectrum of mutant P4 recorded at 378-nm excitation was integrated and compared with the integrated emission spectrum of wild type recorded at 475-nm excitation; both excitation and emission characteristics were corrected.

excitation peak, and shift the emission peak to shorter wavelengths. However, the hypothesized ionizable phenolic group would have to be buried inside the protein at normal pH because the ratio of 471- to 396-nm peaks in the mutants could not be further affected by external pH until it was raised to 10, just below the threshold for denaturation. The pH-sensitivity of wild-type GFP is similar (18).

A fourth mutant, P4, was excitable by UV light and fluoresced bright blue in contrast to the green of wild-type protein (Fig. 4). The excitation and emission maxima were hypsochromically shifted by 14 and 60 nm, respectively, from those of wild-type GFP. The mutated DNA was sequenced and found to contain five amino acid substitutions, only one of which proved to be critical, Tyr-66 → His in the center of the chromophore. The surprising tolerance for substitution at this key residue prompted further site-directed mutagenesis to tryptophan and phenylalanine at this position. Tryptophan gave excitation and emission wavelengths intermediate between tyrosine and histidine (Fig. 3 and Table 1) but was only weakly fluorescent, perhaps due to inefficiency of folding or chromophore formation, whereas phenylalanine gave no detectable fluorescence.

The availability of several forms of GFP with such different excitation and emission maxima [the most distinguishable pair being mutant P4 (Y66H) vs. mutant P11 (I167T)] should facilitate two-color assessment of differential gene expression, developmental fate, or protein trafficking. It may also be possible to use these GFP variants analogously to fluorescein and rhodamine to tag interacting proteins or subunits whose association could then be monitored dynamically in intact cells by fluorescence resonance energy transfer (19, 20). Such fluorescence labeling via gene fusion would be site-specific and would eliminate the present need to purify and label proteins *in vitro* and microinject them into cells.

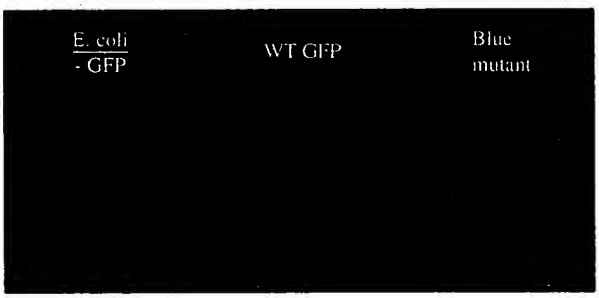


FIG. 4. *E. coli* producing either no GFP (*Left*), wild-type GFP (*Center*), or the P4 mutant (*Right*) in which Tyr-66 is replaced by histidine. Approximately equal quantities of bacteria were suspended in 1-cm cuvettes, excited by a 365-nm transilluminator, and photographed through a low-fluorescence filter passing wavelengths >450 nm. The bacteria producing no GFP were transformed with vector alone. Flecks of green in the two flanking cuvettes are stray reflections from the center cuvette.

1. Wang, Y. L. & Taylor, D. L., eds. (1989) *Methods Cell Biol.* **29.**
2. Peck, K., Stryer, L., Glazer, A. N. & Mathies, R. A. (1989) *Proc. Natl. Acad. Sci. USA* **86,** 4087–4091.
3. Fairchild, C. D. & Glazer, A. N. (1994) *J. Biol. Chem.* **269,** 8686–8694.
4. Ward, W. W. (1979) in *Photochemical and Photobiological Reviews*, ed. Smith, K. C. (Plenum, New York), Vol. 4, pp. 1–57.
5. Cody, C. W., Prasher, D. C., Westler, W. M., Prendergast, F. G. & Ward, W. W. (1993) *Biochemistry* **32,** 1212–1218.
6. Prasher, D. C., Eckenrode, V. K., Ward, W. W., Prendergast, F. G. & Cormier, M. J. (1992) *Gene* **111,** 229–233.
7. Chalfie, M., Tu, Y., Euskirchen, G., Ward, W. W. & Prasher, D. C. (1994) *Science* **263,** 802–805.
8. Inouye, S. & Tsuji, F. I. (1994) *FEBS Lett.* **341,** 277–280.
9. Wang, S. & Hazelrigg, T. (1994) *Nature (London)* **369,** 400–403.
10. Sikorski, R. S. & Boeke, J. D. (1991) *Methods Enzymol.* **194,** 302–318.
11. Muhlrad, D., Hunter, R. & Parker, R. (1992) *Yeast* **8,** 79–82.
12. Sambrook, J., Fritsch, E. F. & Maniatis, T. (1989) *Molecular Cloning: A Laboratory Manual* (Cold Spring Harbor Lab. Press, Plainview, NY), 2nd Ed., pp. 17.37–17.41.
13. Ward, W. W. & Bokman, S. H. (1982) *Biochemistry* **21,** 4535–4540.
14. Kidwai, A. R. & Devasia, G. M. (1962) *J. Org. Chem.* **27,** 4527–4531.
15. Kjaer, A. (1953) *Acta Chem. Scand.* **7,** 1030–1035.
16. Merbs, S. L. & Nathans, J. (1992) *Science* **258,** 464–466.
17. Ward, W. W. (1981) in *Bioluminescence and Chemiluminescence*, eds. DeLuca, M. A. & McElroy, W. D. (Academic, New York), pp. 235–242.
18. Ward, W. W., Prentice, H. J., Roth, A. F., Cody, C. W. & Reeves, S. C. (1982) *Photochem. Photobiol.* **35,** 803–808.
19. Adams, S. R., Harootunian, A. T., Buechler, Y. J., Taylor, S. S. & Tsien, R. Y. (1991) *Nature (London)* **349,** 694–697.
20. Adams, S. R., Bacskai, B. J., Taylor, S. S. & Tsien, R. Y. (1993) in *Fluorescent Probes for Biological Activity of Living Cells: A Practical Guide*, ed. Mason, W. T. (Academic, New York), pp. 133–149.